Metallographic Examination of White etching Cracks in Bearing Steels

Matthew Petersen

August 26, 2016

Contents

1 Abstract

White etching cracks are the leading cause of premature wind turbine gearbox bearing failure. This paper presents work done to replicate white etching cracks at a benchtop scale in a controlled laboratory environment. A three-ring-on-roller micro pitting rig was used to induce white etching crack formation, and standard metallographic sectioning procedures were used to image both laboratory test samples and failed wind turbine gearbox bearing samples. The white etching cracks formed in test rollers were shown to be substantially similar to those formed in the field in wind turbine components, and the images collected provide valuable data for determining the factors leading to white etching crack formation.

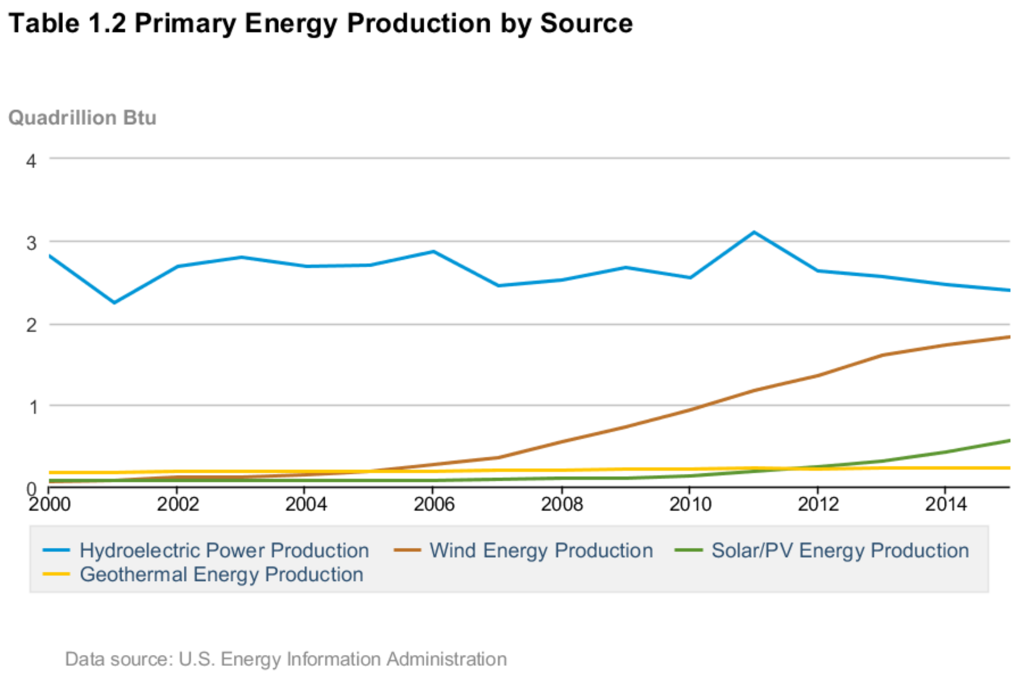

Figure 1: Global Renewable Energy Production by Source[1]

2 Introduction

Wind energy is the fastest growing form of renewable energy, outpacing solar, hydroelectric and other renewable sources in its rate of growth over the past decade, as can be seen in figure 1. Clean and efficient, wind turbines are being installed globally in ever-larger numbers. In 2015, wind power surged dramatically, adding 8598MW of new capacity and investing $14.5 billion. Cumulative wind capacity grew by 12%, to a total of 73992MW. This growth also represented the largest source of electric-generating capacity growth in 2015, constituting 41% of total additions[2].

However, while the industry may be growing healthily, many wind turbines themselves are stricken with mechanical difficulties linked to premature bearing failure. The gearboxes that wind turbines use are subject to hostile conditions and infrequent maintenance, with bearings inside experiencing torque reversals, heavy loads, and frequent starting and stopping. The drivetrain converts the low speed rotation of the rotor, in the range of 13-20 rpm, to the high speed rotation needed for electricity generation of 1600

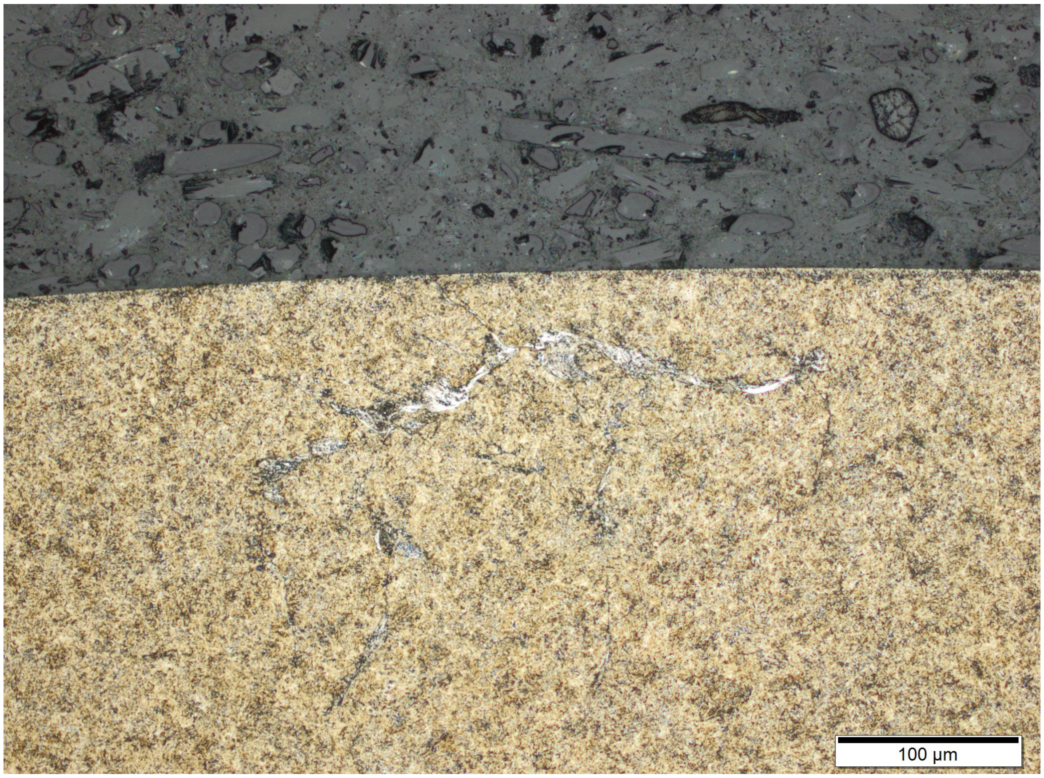

Figure 2: White etching crack

rpm. Many other mechanical systems also contain bearings, such as the main rotor shaft, the generator itself, and the blade pitch drives, along with others. Wind turbine gearbox bearings (WTGB) experience frequent premature failure, predominantly due to white etching cracks (WEC). WEC lead to bearing failure at just a small fraction of the design life of the bearing, with lifetimes ranging from 1-20% of the design life[6]. Design life here means the L_{10} bearing design life calculated for standard rolling contact fatigue (RCF).

White etching cracks are characterized by a white appearance when etched with nital, indicative of grain refinement at the nanoscale[5] (see figure 2). This white etching area consists of nano-ferrite grains, and possesses a hardness 30-50% higher than the bulk material around it[6]. The cracks are associated with spalls and pits on the bearing surface; see figure 3. However, the surface features associated with WEC differ from those associated with RCF and conventional material decay[6]. The mechanism of WEC formation

Figure 3: Failed wind turbine gearbox bearing (inner raceway, high speed shaft)

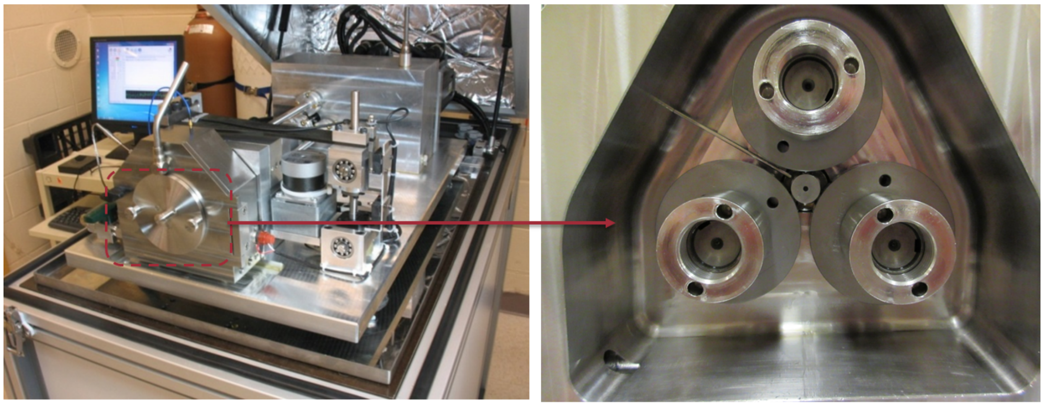

Figure 4: MPR Setup[5]

is unclear, and many competing theories exist to explain this phenomenon, with possible driving forces including various hydrogen embrittlement mechanisms, operational transients such as impact loads, and electrical effects[3]. The current work aims to replicate WEC in a controlled laboratory environment, and characterize the cracks formed in both the lab and in the field.

3 Methods

3.1 Replication of WEC

A test methodology for the replication of WEC was developed making use of a PCS Instruments three-ring-on-roller micro pitting rig (MPR), as can be seen in figure 4. Specimens were supplied by PCS instruments, and manufactured out of AISI 52100 through-hardened martensitic steel. The MPR allowed many contact parameters to be controlled, including temperature, load and slide-to-roll ratio. Each of these parameters could be varied over a wide range; slide-to-roll ratio from pure rolling to pure sliding, load from 0.5 to 3GPa at the contact, and temperature up to 100°C by the use of a control loop operating a resistive heater and a convective cooler in tandem. A fully-formulated gear oil was used for lubrication. Before each test, the specimens and MPR chamber were cleaned with a series of solvents. Each test consumed one roller, while one set of rings could be used for up to two tests. Images as well as optical profilometry datasets were collected for rings and rollers at various points around their circumference. Load was applied to the specimen via the top ring, and strain measurements on the loading arm were used to calculate displacements, and hence accelerations, of the top ring itself. Peak-to-peak acceleration was used as a cutoff parameter for the MPR: when acceleration amplitude reached a threshold value, the MPR tripped, stopping the machine at a point when significant surface damage was likely to have occurred. This method also established a baseline lifetime for failure.

3.2 Characterization of WEC

In order to characterize the morphology of WEC, standard metallographic methods were employed. Rollers, after being used in MPR trials, were cut on a low-speed saw using a carbide wafering blade. Low-magnification images were taken at 90°intervals around the roller, as well as at any points of interest, such as spalls or cracks. These images allow for the distance to the wear track from the edge of the cut to be determined. A manufacturing mark on the roller was used as a datum. The roller was then mounted in a two-part resin puck - a layer around the roller impregnated with glass for edge retention, and a filler layer of pure resin elsewhere. The puck was labeled with the same datum mark used for the previous imaging. Material was then removed using a grinding wheel until the edge of the wear track was near, using a series of Rockwell hardness tester indents as depth measurements. When the wear track was reached, a series of diamond slurries (9µm, 3µm, 1µm) were used to polish the puck and roller to a mirror finish. All polishing and grinding work was performed using a Struers TegraPol automatic polishing machine. The surface was then cleaned with isopropanol, and etched with standard Nital solution.

A similar process was used for sectioning WTGB specimens, with the caveat that WTGB specimens required longer polishing times due to their larger size. WTGB specimens were taken from the inner ring of cylindrical roller bearings from the high speed shaft of a wind turbine. These samples were received as whole bearing components, with dimensions on the order of several inches. Smaller chunks were cut out of the rings, and these were the pieces mounted in resin pucks. The pieces were mounted axially, with the axis of rotation parallel to the central axis of the puck.

Each sample was examined with a measuring microscope. The amount of material removed was determined by comparing the depth of the Rockwell indent at this point to the depth at the previous section. Each sample, roller or WTBG, was surveyed over the extent of the wear track, with care being taken to image, usually at 20x and 50x magnification, any points of interest, such as the surface features viewed before mounting, as well as subsurface cracks and inclusions not seen from the exterior of the sample. The polishing and imaging processes were repeated multiple times for each sample at various spacings, depending on the features of the sample in question.

4 Results & Discussion

The MPR methodology has allowed for wide ranges of conditions to be replicated at a benchtop scale, with many different controllable parameters. Tests were conducted with a wide range of loads, temperatures, and test formats: some tests included a run-in period, and others did not. The experimental cut-off method based on acceleration worked well, and repeatably stopped the test shortly after major damage occurred, in the form of spalls or large amounts of micro-pitting. In the cases where the cut-off did not trip, a time-out came into effect whereby the test was stopped after a large number of cycles. This was the case in several tests, where either the number of cycles to failure was underestimated or the type of failure generated was not associated with high accelerations.

The sectioning methods described above yielded many high quality images of WEC, both in test rollers and in WTGB specimens. The cracks themselves had many characteristics in common. Both sets of cracks, roller and WTGB, exhibited similar branching structures, and were located at similar depths, as can be seen in figures 5 and 6. The subsurface nature of the cracks is a key feature, marking out the crack as being initiated by something other than surface damage. In addition, in both classes of sample, cracks were often found without nucleating inclusions. This is notable because it points to a source of cracking other than stress concentration in at least some cases.

One difference between tests, appearing in both WTGB and roller samples, was the thickness of the white etching area (WEA) around the cracks. As figure 6 shows, some cracks exhibited a thin WEA extending a short distance, no more than a few microns, from the crack itself. Others, as in figure 5, had a thicker, more extensive layer, with greater irregularity in WEA breadth. This did not appear to occur more commonly in either roller or WTGB samples when compared to the other, and so may reflect some other effect upon WEC formation that is yet to be determined.

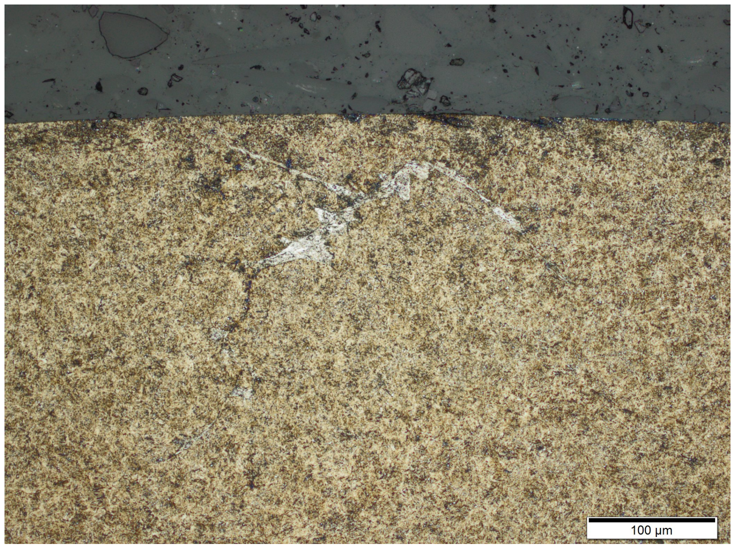

(a) 20x magnification

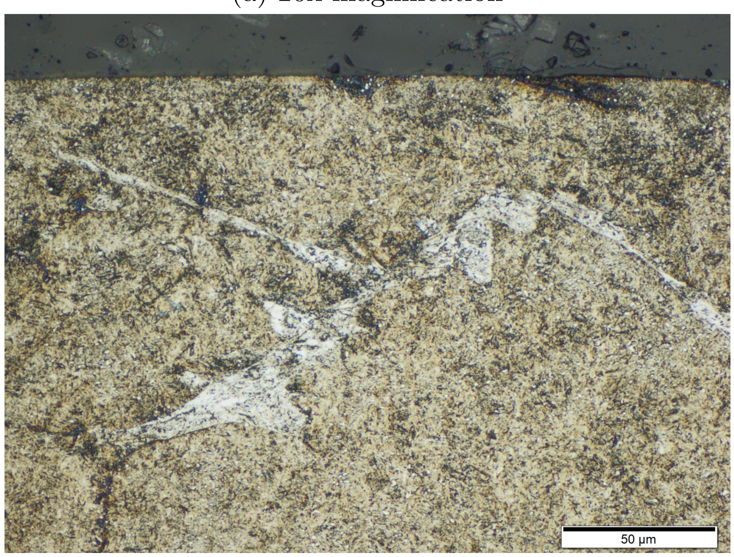

(b) 50x magnification

Figure 5: WEC in roller 160715, 30°location

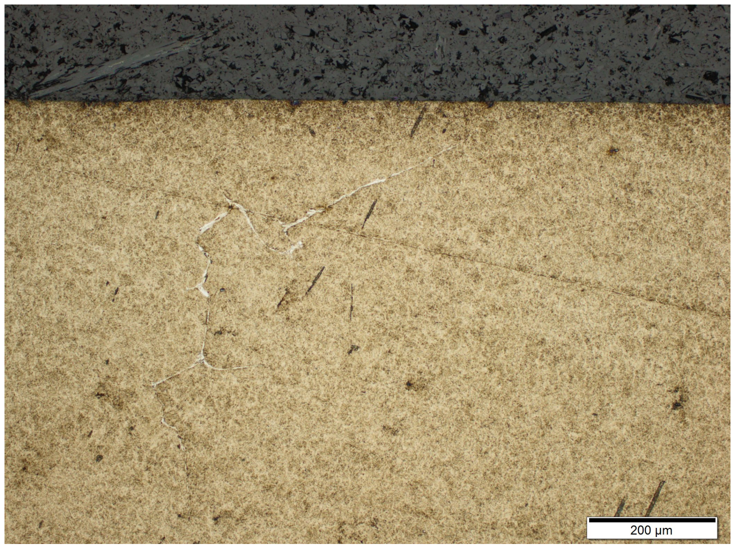

(a) 10x magnification

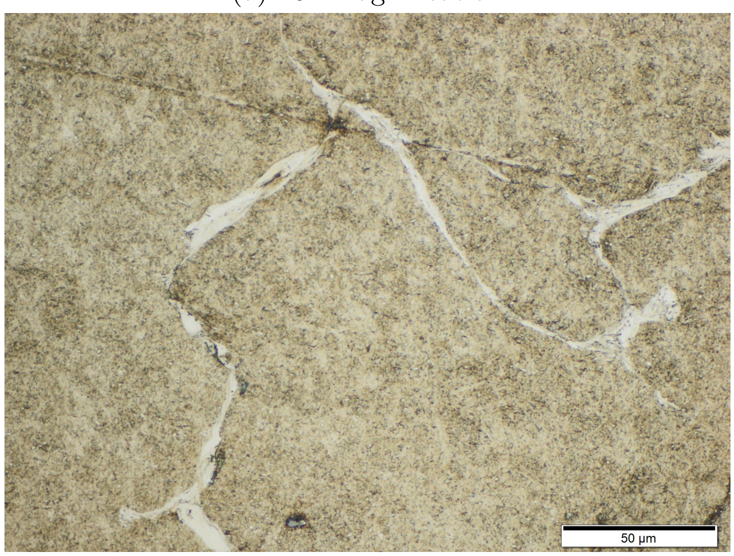

(b) 50x magnification

Figure 6: WEC in wind turbine sample

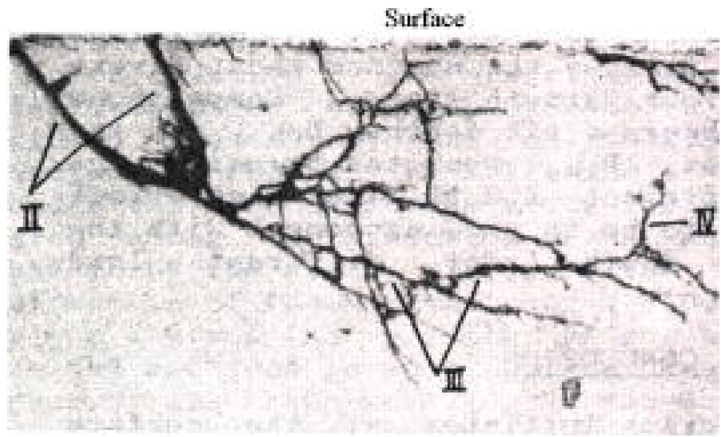

Figure 7: Crack from rolling contact fatigue; figure after [7]

The testing is also useful in comparing the cracks formed as WEC to those formed as the result of rolling contact fatigue. Crack networks formed by RCF occasionally present as dense networks of cracks, with many branches reaching the surface. Often, the cracks also exhibit a directional tendency related to the over-rolling direction. In the case of WEC, cracks almost never formed dense networks as seen in figure 7, and when interacting with the surface, often only connected at one location, usually a spall or pit. This reinforces the clear distinction between RCF cracks and WEC.

Overall, the WEC found in both roller and WTGB specimens had similar features. This validates the use of the MPR apparatus for WEC replication purposes. Other work has used samples pre-charged with hydrogen[5], which, while readily inducing WEC formation, does not accurately represent real contact conditions. The MPR allows for full control over a wide range of contact conditions, and can generate WEC without extensive sample preparation, such as the aforementioned charging. In addition, the sectioning methods used in this study allow confirmation of the presence of WEC through etching, and provide an easy way to compare cracks developed in the lab to those formed in the field.

References

[1] U.S. Energy Information Administration. *Monthly Energy Review July 2016*. 2016.

[2] U.S. Department of Energy EERE. *2015 Wind Technologies Market Report*. Aug. 2016.

[3] M.-H. Evans. "An updated review: white etching cracks (WECs) and axial cracks in wind turbine gearbox bearings". In: *Materials Science and Technology* 32 (2016), pp. 1–37. DOI: 10.1080/02670836.2015.1133022.

[4] M.-H. Evans et al. "White etching crack (WEC) investigation by serial sectioning, focused ion beam and 3-D crack modelling". In: *Tribology International* 65 (2013). 39th Leeds-Lyon Symposium on Tribology Special Issue: Great Challenges in Tribology, pp. 146–160. DOI: 10.1016/j.triboint.2013.03.022.

[5] Benjamin Gould and Aaron Greco. "Investigating the Process of White Etching Crack Initiation in Bearing Steel". In: *Tribology Letters* 62.2 (2016), pp. 1–14. ISSN: 1573-2711. DOI: 10.1007/s11249-016-0673-z.

[6] A. Greco et al. "Material wear and fatigue in wind turbine Systems". In: *Wear* 302.1-2 (2013), pp. 1583–1591. DOI: 10.1016/j.wear.2013.01.060.

[7] F. Sadeghi et al. "A Review of Rolling Contact Fatigue". In: *Journal of Tribology* 131.4 (2009). DOI: 10.1115/1.3209132.